Streaming Potential in Microflows and Nanoflows

Jeevanjyoti Chakraborty and Suman Chakraborty

Abstract In this chapter, we discuss a wide variety of important effects due to streaming potential when fluid flow takes place through conduits of micro- and nanometric dimensions. We first introduce this as one of the four primary electrokinetic phenomena with suitable background, and describe its significance in numerous natural and engineered settings. Its practical usage and measurement being inordinately linked to predictive models, we present the theory behind streaming potential. In light of recent research findings, and recognizing their importance in micro- and nano-flows, we also highlight the influence of streaming potential when considered together with the consideration of hydrophobic, steric, and thermal effects.

Keywords Streaming potential · Electrokinetics · Hydrophobic effects · Steric effect · Soret effect · Thermoelectric effect

1 Introduction

The colloidal scientist is perennially concerned with the charge of the particles (s)he is handling as this charge is of paramount importance in determining the stability of the dispersion and its overall behavior. The geophysicist interested in a

J. Chakraborty · S. Chakraborty (✉)
Advanced Technology Development Centre, Indian Institute of Technology Kharagpur, Kharagpur 721302, West Bengal, India
e-mail: sumanchakraborty_iitkgp@yahoo.com

J. Chakraborty
Mathematical Institute, University of Oxford, Oxford OX2 6GG, UK

S. Chakraborty
Mechanical Engineering Department, Indian Institute of Technology Kharagpur, Kharagpur 721302, West Bengal, India

K. J. Vinoy et al. (eds.), *Micro and Smart Devices and Systems*,
Springer Tracts in Mechanical Engineering, DOI: 10.1007/978-81-322-1913-2_20,

broad spectrum of sub-surface investigations ranging from the mapping of pore geometry to the exploration of alternative energy sources based on harnessing geothermal energy reserves, needs to take recourse to ingenious methods that exploit underground fluid flow in newer forms. Soil and mining engineers are interested in various dewatering and decontamination processes. In a starkly different realm, biophysicists are increasingly interested in unraveling the fundamental mechanisms through which bone responds to external stress via its interaction with interstitial fluids. The membrane scientist needs to take into account the various factors contributing to the specific filtration process (s)he is trying to develop. The motivation for such developments stems from the sophistication (as far as membranes go) found in the sheath of cells, and in sub-cellular entities. The researcher trying to develop lab-on-a-chip devices at the micro- and nanoscales needs alternative fluid actuation mechanisms, or even when using traditional pressure-driven ones needs to take into consideration additional factors which might be of tremendous consequence. The common thread that binds the interests and motivation of the aforementioned scientists and engineers is the physicochemical phenomenon where the boundary layer between one charged phase and another undergoes a shearing process. This phenomenon is manifested in many different forms in various settings, and is broadly referred to as electrokinetics. In this chapter, we focus on one such particular form called the streaming potential that lies at the very core of understanding electrokinetics in different contexts.

1.1 Understanding Streaming Potential

1.1.1 The Electrical Double Layer (EDL) and Electrokinetics

The most important point to note regarding electrokinetic phenomena is that they are critically dependent on the establishment of an electrified interface between two phases, one of which is usually a solid. The first step in the formation of such an electrified interface is the generation of a surface charge. Various mechanisms through which such charge is generated include an imbalance in the number of crystal lattice cations or anions on the surface, crystal lattice defects, surface dissociation, and ion adsorption from solutions; the mechanism may also be some combination of these.

This surface charge is invariably accompanied by the presence of certain ionic species in the adjacent liquid medium. The ions in the solution of opposite charge to that of the surface are referred to as counterions while the ions of like charges are referred to as co-ions. It is intuitive to expect that the counterions would be attracted towards the surface while the co-ions would be repelled by it. If the Coulombic forces were the only factors, the counterions would stack up against the surface—thus, perfectly shielding the rest of the ions in the solution. Such a scenario is precluded, however, by the random thermal motion of the ions at any

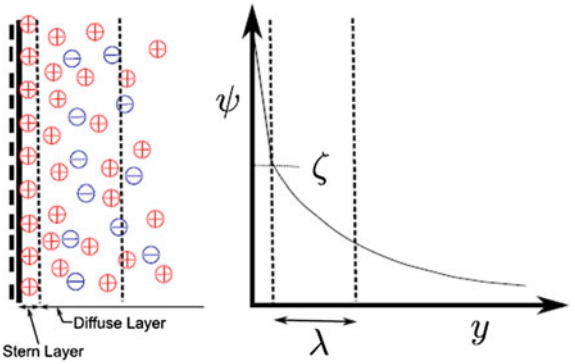

Fig. 1 Structure of the EDL and the distribution of the electric potential

finite temperature. As a result of interplay between the Coulombic forces and the thermal motion a distribution of the counterions and the co-ions is established in the vicinity of the charged surface. In this distribution, the counterions outnumber the co-ions in such a way that the charge imbalance resulting from it is perfectly neutralized by the charge on the surface. It is the surface electric charge together with the balancing charge in the solution that constitutes the electrified interface. This is referred to as the electrical double layer [1] or EDL, in short.

In the most widely accepted model for the structure of the EDL (the Guoy-Chapman-Stern model) there is a monolayer of counterions that stays attached to the charged surface (see Fig. 1). This is called the Stern layer, or the compact layer, or the Helmholtz layer. Just adjacent to the edge of the Stern layer is the shear plane. The potential at the edge of the Stern layer is called the zeta potential. The part of the EDL beyond this shear plane is called the diffuse layer because it is susceptible to motion when the fluid is sheared past the charged surface by any external actuation. The characteristic thickness of the EDL is defined to be the position from the wall where the potential drops to $1/e$ (e being the Euler number) of the zeta potential value; this characteristic thickness is referred to as the Debye length. As noted earlier, this shearing motion of the diffuse part of the electrified interface across the charged surface is what gives rise to a host of electrokinetic phenomena, the primary four among which are electroosmosis, electrophoresis, streaming potential, and sedimentation potential.

1.1.2 Origin of the Streaming Potential

When a pressure-gradient (or any other mechanical actuation) is used to set the liquid in a capillary tube (or channel) or a porous plug in motion, the diffuse part of the double layer also moves along with the flow and is sheared past the charged surface. The current that is generated as a result of the advection of the ions is called streaming current. The consequent transfer of ions downstream gives rise to an electric field in the opposite direction. The potential associated with this electric field opposes the streaming current. This happens through a back

conduction of ions, and also through an electroosmotic flow to a certain extent. This current directed opposite to the streaming current is called the leak current. The term "conduction current" is often used in a sense that subsumes within it both the mechanisms of the back flow of the ions. After a very short time, a dynamic equilibrium condition is reached when the leak current balances the streaming current so that the total ionic current across the confinement through which the fluid flow is taking place is zero. The potential difference measured across the conduit in this condition is known as the streaming potential.

1.2 Many Uses of the Streaming Potential

The phenomenon of streaming potential was discovered by Georg Quincke, who first observed that he could measure an electrical potential difference between the ends of a tube when he pumped water through it [2]. Since then, streaming potential has come to be used in a wide variety of settings as outlined in the opening paragraph of Sect. 1. It is a standard practice to determine the zeta potential of various surfaces using streaming potential or streaming current measurements [3]. In the geophysical realm techniques based on downhole measurements of streaming potential are developed to monitor fluid flows in hydrocarbon reservoirs or oil fields. More generally, there is a great interest in the geophysical community on streaming potential measurements for use in pore geometry determination, for monitoring underground fluid flow, and rock/fluid interfacial chemistry [4]. Additionally, streaming potential may help in monitoring and prediction of earthquakes [5]. The study of streaming potentials at elevated temperature and pressure may also be used for geothermal exploration. These have implications in the study of volcanoes [6]. In the physiological realm, the mechanism behind how bones respond via interstitial fluid flow to external loading is believed to be based on streaming potential [7]. Streaming potential may also be able to sensitively indicate intervertebral disk degeneration [8]. In the context of filtration processes, streaming potential can be used to study the influence that fouling phenomena has on membrane surface properties [9]. A comprehensive discussion on these various aspects may be found in Ref. [10].

In this chapter, we particularly focus on studies of streaming potential mediated flows at micro- and nanofluidic scales. The motivation behind this is as follows. Streaming potential phenomena in narrow confinements is important from the perspective of a wide variety of practical applications encompassing the lab-on-a-chip (LOC) technology. A critical point to note is that LOC fluidic technology is inspired by electronic integrated circuits (interestingly, it is from "electronics" that the term "fluidic" is coined). LOC systems are created by using chip-based micromachining techniques to shrink the size of fluid handling systems aimed at improving chemical and biological analysis. Thus, this technology mimics both the fabrication technology and the overall "smaller, cheaper, faster" paradigm of the integrated circuit industry. Furthermore, just as "wires" form the basic pathways

in electrical/electronic circuits, micro- and nanofluidic channels are the most fundamental structures in LOC devices [11]. These not only offer suitable settings to study the fundamental physics behind the fluidic phenomena increasingly influenced by surface effects in general, and electrokinetics, in particular, but also provide a basis for the design of practical devices [12–16]. A theoretical consideration of such channel-like geometries may serve as a good model for certain apparently complicated physical setups that are, however, characterized by symmetries or other possibilities for geometrical simplifications.

Based on the above, we present a general theoretical description of streaming potential in Sect. 2. With this background, we then present, in the rest of the chapter, an outline of the motivation of, and findings from a few recent investigations that were carried out to understand the combined influence of streaming potential and certain other physico-chemical phenomena on micro-/nanoscale fluid flows.

2 Mathematical Model of Streaming Potential

We consider the model problem of streaming potential flow of a binary symmetric electrolyte through a straight channel having either a slit or circularly symmetric cross-section. The characteristic dimension in either cross-section, generally represented by R, is considered to be much smaller than the channel length L. The fluid is primarily actuated by a pressure gradient. In the absence of surface heterogeneities, the resulting velocity field may be safely considered to be unidirectional so that $\boldsymbol{u} = u\hat{\boldsymbol{e}}_x$ where $\hat{\boldsymbol{e}}_x$ is the unit vector along the axial direction. The origin is located at the centerline of the channel. The surface is considered to be negatively charged; the counterions and the co-ions are, respectively, identified by the "+" and "−" subscripts. The valences are given by $z_+ = -z_- = z$. Then, for the case of steady flow, the species transport equation reduces to

$$-\nabla\cdot\left(D_\pm\nabla n_\pm \pm \frac{ze}{k_BT}D_\pm n_\pm\nabla\varphi\right) + \nabla\cdot(n_\pm\boldsymbol{u}) = 0, \tag{1}$$

where $D_\pm$ refers to the diffusivity of the cation, and the anion. To address the cases of the slit channel and the circular channel simultaneously in the same framework, we use a general representation. Toward that end, for the differential operators we follow the notation of Stone [17]. Thus, the gradient operator is represented by $\nabla \equiv \frac{\partial}{\partial\xi}\hat{\boldsymbol{e}}_\xi + \frac{\partial}{\partial x}\hat{\boldsymbol{e}}_x$, where ξ is the general coordinate transverse to the wall; and the divergence by $\nabla\cdot\square = \frac{1}{\xi^{d-1}}\frac{\partial}{\partial\xi}\left(\xi^{d-1}\square_\xi\right) + \frac{\partial}{\partial x}\square_x$, where $d = 1$ for the slit cross-section, and $d = 2$ for the circularly symmetric cross-section. Anticipating the use of the Laplacian operator, we also note $\nabla^2 = \frac{1}{\xi^{d-1}}\frac{\partial}{\partial\xi}\left(\xi^{d-1}\frac{\partial}{\partial\xi}\right) + \frac{\partial^2}{\partial x^2}$. We use the non-dimensional variables $\tilde{\xi} = \frac{\xi}{\mathcal{R}}$, $\tilde{x} = \frac{x}{\mathcal{L}}$, $\tilde{n}_\pm = \frac{n_\pm}{n_0}$, $\tilde{\varphi} = \frac{ez\varphi}{k_BT}$, $\tilde{\boldsymbol{u}} = \frac{u\hat{\boldsymbol{e}}_x}{\mathcal{U}}$, where n_0 is

the number density of both the counterions, and the co-ions in the bulk, and $\boldsymbol{U}$ is the scale of the unidirectional velocity along the axial direction. Further, considering $D_+ = D_- = D$ to be spatially invariant, Eq. (1) reduces in non-dimensional form to

$$\begin{aligned} &-\frac{1}{\tilde{\xi}^{d-1}}\frac{\partial}{\partial\tilde{\xi}}\left(\tilde{\xi}^{d-1}\frac{\partial\tilde{n}_\pm}{\partial\tilde{\xi}}\right)+\left(\frac{\mathcal{R}}{\mathcal{L}}\right)^2\frac{\partial^2\tilde{n}_\pm}{\partial x^2}+Pe\left(\frac{\mathcal{R}}{\mathcal{L}}\right)\frac{\partial}{\partial x}(\tilde{n}_\pm\tilde{u}) \\ &\mp\left[\frac{1}{\tilde{\xi}^{d-1}}\frac{\partial}{\partial\tilde{\xi}}\left(\tilde{\xi}^{d-1}\tilde{n}_\pm\frac{\partial\tilde{\varphi}}{\partial\tilde{\xi}}\right)+\left(\frac{\mathcal{R}}{\mathcal{L}}\right)^2\frac{\partial}{\partial x}\left(\tilde{n}_\pm\frac{\partial\tilde{\varphi}}{\partial x}\right)\right]=0, \end{aligned} \tag{2}$$

where $Pe=\frac{\mathcal{U}\mathcal{R}}{D}$ is the ionic species Péclet number. This may be viewed as the product of the Reynolds number $Re=\mathcal{U}\mathcal{R}/\upsilon$ (where $\upsilon=\eta/\rho$ is the kinematic viscosity with η being the dynamic viscosity, and ρ the density of the fluid) and the Schmidt number $Sc=\upsilon/D$. The small value of $Re(\ll 1)$, very common in micro- and nanofluidic settings, does not necessarily ensure that Pe is small because Sc which represents the strength of the momentum diffusivity relative to the species diffusivity may be significantly larger than unity. For instance, with typical ionic diffusivities, D, are of the order of 10^{-9} $\mathrm{m^2s^{-1}}$, in aqueous solutions where $\upsilon\sim 10^{-6}$ $\mathrm{m^2s^{-1}}$, $Sc\sim\mathcal{O}(10^3)$. It is then possible for $Pe\gtrsim\mathcal{O}(1)$. However, it is because Pe is multiplied by the factor $(\mathcal{R}/\mathcal{L})$ that the advective contribution may indeed be safely neglected as long as $\mathcal{R}\ll\mathcal{L}$. Similarly, other terms multiplied by the factor $(\mathrm{R/L})^2$ may also be neglected—thus, clearly indicating that gradients along the axial direction have negligible contribution. We further note that $\varphi=\psi-xE_S$, where E_s is the spatially invariant electric field. Thus, Eq. (2) becomes

$$\frac{1}{\tilde{\xi}^{d-1}}\frac{\partial}{\partial\tilde{\xi}}\left(\tilde{\xi}^{d-1}\frac{\partial\tilde{n}_\pm}{\partial\tilde{\xi}}\right)\pm\frac{1}{\tilde{\xi}^{d-1}}\frac{\partial}{\partial\tilde{\xi}}\left(\tilde{\xi}^{d-1}\tilde{n}_\pm\frac{\partial\tilde{\varphi}}{\partial\tilde{\xi}}\right)=0. \tag{3}$$

By integrating once and using the symmetry condition at the centerline, we get

$$\partial(\ln\tilde{n}_\pm)/\partial\tilde{\xi}=\mp\partial\tilde{\psi}/\partial\tilde{\xi}. \tag{4}$$

This is essentially the same equation that leads to the Boltzmann distribution in the purely equilibrium case. Thus, we can understand that the fluid flow does not affect the equilibrium structure of the EDL in the case of a pressure-gradient-driven flow through straight channels with large aspect ratios $(\mathcal{R}\ll\mathcal{L})$. This is complemented by the Poisson equation written for the present setting in a reduced and dimensionless form as

$$\frac{1}{\tilde{\xi}^{d-1}}\frac{\partial}{\partial\tilde{\xi}}\left(\tilde{\xi}^{d-1}\frac{\partial\tilde{\psi}_\pm}{\partial\tilde{\xi}}\right)=-\left(\frac{\mathcal{R}^2e^2z^2n_0}{\varepsilon k_BT}\right)\tilde{\rho}_e, \tag{5}$$

where the charge density, ρ_e, has been non-dimensionalized by ezn_0. The fluid velocity is governed by the x-direction component of the Navier-Stokes equation, which for the steady case is written as

$$\rho\left(u\frac{\partial u}{\partial x}\right) = -\frac{\partial p}{\partial x} + \eta\left[\frac{1}{\xi^{d-1}}\frac{\partial}{\partial \xi}\left(\xi^{d-1}\frac{\partial u}{\partial \xi}\right) + \frac{\partial^2 u}{\partial x^2}\right] + \rho_e E_S, \tag{6}$$

where $\rho_e E_S$ is the electrokinetic body force exerted on a unit volume of the fluid due to the streaming potential electrical field E_s. In non-dimensional terms, this is written as

$$\begin{aligned} Re\left(\frac{\mathcal{R}}{\mathcal{L}}\right)\tilde{u}\frac{\partial \tilde{u}}{\partial \tilde{x}} = &-\frac{\mathcal{R}^2 \Delta p}{\eta \mathcal{L}\mathcal{U}}\frac{\partial \tilde{p}}{\partial \tilde{x}} + \frac{1}{\tilde{\xi}^{d-1}}\frac{\partial}{\partial \tilde{\xi}}\left(\tilde{\xi}^{d-1}\frac{\partial \tilde{u}}{\partial \tilde{\xi}}\right) \\ &+ \left(\frac{\mathcal{R}}{\mathcal{L}}\right)^2\frac{\partial^2 \tilde{u}}{\partial \tilde{x}^2} - \frac{\varepsilon k_B T E_0}{\eta e z \mathcal{U}}\frac{1}{\tilde{\xi}^{d-1}}\frac{\partial}{\partial \tilde{\xi}}\left(\tilde{\xi}^{d-1}\frac{\partial \tilde{\psi}}{\partial \tilde{\xi}}\right)\tilde{E}_S \end{aligned}. \tag{7}$$

The inertial term on the left-hand side in the preceding equation is clearly negligible because both Re and $(\mathcal{R}/\mathcal{L})$ are very small. The term involving the pressure-gradient is the primary actuator of the flow. Hence, the velocity scale $\boldsymbol{U}$ is set by considering this term to be $\mathcal{O}(1)$, giving $\mathcal{U} \sim \left(\mathcal{R}^2/\eta\right)(\Delta p/\mathcal{L})$. The viscous term with the prefactor $(\mathrm{R/L})^2$ is also neglected. The streaming potential field is non-dimensionalized by an appropriate scale E_0 (to be explicated later). Then, Eq. (7) reduces to

$$-1 + \frac{1}{\tilde{\xi}^{d-1}}\frac{\partial}{\partial \tilde{\xi}}\left(\tilde{\xi}^{d-1}\frac{\partial \tilde{u}}{\partial \tilde{\xi}}\right) - \mathcal{A}\frac{1}{\tilde{\xi}^{d-1}}\frac{\partial}{\partial \tilde{\xi}}\left(\tilde{\xi}^{d-1}\frac{\partial \tilde{\psi}}{\partial \tilde{\xi}}\right)\tilde{E}_S = 0, \tag{8}$$

where $\mathcal{A} = (\varepsilon k_B T E_0)/(\eta e z \mathcal{U})$. By integrating once, and using the symmetry condition at the channel centreline, we have

$$\frac{\tilde{\xi}}{d} + \frac{\partial \tilde{u}}{\partial \tilde{\xi}} - \mathcal{A}\frac{\partial \tilde{\psi}}{\partial \tilde{\xi}}\tilde{E}_S = 0. \tag{9}$$

By integrating again, and using the no-slip boundary condition $\tilde{u} = 0$ and $\tilde{\psi} = \tilde{\zeta}$ (the non-dimensional value of the zeta potential) at $\tilde{\xi} = 1$ (the wall), we have

$$\tilde{u} = \frac{1}{2d}\left(1 - \tilde{\xi}^2\right) + \mathcal{A}\tilde{E}_S\left(\tilde{\psi} - \tilde{\zeta}\right). \tag{10}$$

The condition used to determine the as-yet-unknown streaming potential field is to set the total ionic current across any cross-section to zero. This is given by

$$\int_{-\mathcal{R}}^{\mathcal{R}} \left(j_{+x}\hat{\boldsymbol{e}}_x - j_{-x}\hat{\boldsymbol{e}}_x\right) \cdot \hat{\boldsymbol{e}}_x (2\pi\xi)^{d-1} d\xi = 0, \tag{11}$$

where $j_{\pm x} = -D\frac{\partial n_\pm}{\partial x} \mp D\frac{ez}{k_B T} n_\pm \frac{\partial \varphi}{\partial x} + n_\pm u$ represents the flux of the counterions, and the co-ions in the x-direction. It follows directly from Eq. (4) that the ionic distributions are practically invariant along the x-direction. Then, the contribution of the $\partial n_\pm/\partial x$ term to the flux is taken to be negligible. Again, we note that $\varphi = \psi - xE_S$. But just like the ionic distribution, the contribution of $\partial\psi/\partial x$ to the flux is also negligible. With these simplifications, together with expanding the expression of u from Eq. (10), and non-dimensionalization, we get

$$\int_{-1}^{1} \left[\begin{array}{c} (\tilde{n}_+ - \tilde{n}_-)\left\{\frac{1}{2d}\left(1 - \tilde{\xi}^2\right) + \mathcal{A}\,\tilde{E}_S\left(\tilde{\psi} - \tilde{\zeta}\right)\right\}\mathcal{U} \\ + \frac{ezD}{k_B T}(\tilde{n}_+ + \tilde{n}_-)\tilde{E}_S E_0 \end{array} \right] \tilde{\xi}^{d-1} d\tilde{\xi} = 0, \tag{12}$$

from which we get the nondimensional streaming potential field as

$$\tilde{E}_S = \frac{I_1}{I_2 + \mathcal{K} I_2}, \tag{13}$$

where $I_1 = \frac{1}{2d}\int_{-1}^{1} (\tilde{n}_+ - \tilde{n}_-)\left(1 - \tilde{\xi}^2\right)\tilde{\xi}^{d-1} d\tilde{\xi}$, $I_2 = \int_{-1}^{1} (\tilde{n}_+ + \tilde{n}_-)\tilde{\xi}^{d-1} d\tilde{\xi}$, $I_3 = \int_{-1}^{1} \left(\tilde{\psi} - \tilde{\zeta}\right)(\tilde{n}_+ - \tilde{n}_-)\tilde{\xi}^{d-1} d\tilde{\xi}$, and $\mathcal{K} = \frac{\varepsilon k_B^2 T^2}{\eta e^2 z^2 D}$. We note that the scale of the streaming potential field has been set as $E_0 = -\frac{k_B T}{ezD}\frac{R^2}{\eta}\left(\frac{\Delta p}{L}\right)$. Using these in Eq. (10) gives us the velocity of the fluid flow.

3 Combined Influence of Streaming Potential and Other Effects

Notwithstanding the wide spectrum of research contributions in flows influenced by streaming potential in micro- and nanochannels, certain important aspects have remained largely unexplored until recently. In the rest of this chapter, we present a brief overview of some recent investigations that explore the concerted influence of streaming potential and certain other micro-/nanoscale physicochemical phenomena on fluid flows at such length scales.

3.1 Hydrophobic Effects

While the influence of hydrophobic effects on microscale flows in general and electrokinetic flows in particular have been studied widely, such influence is often relegated to the boundary conditions in the form of a specified slip-length. Notwithstanding the widespread success of this approach, a slip-length-based modeling framework cannot, however, resolve the actual physical mechanism through which such hydrophobic effects give rise to an overall reduction in the resistance to the fluid flow: indeed, such reduction fundamentally arises because the hydrophobic substrate induces the depletion of the fluid in the near wall region thus allowing the bulk fluid to smoothly slide over a smoothening blanket of the depleted phase with reduced viscosity.

Departing from the traditional approaches, in a recent investigation [18], we model this depletion mechanism through a phase-field model by expressing the viscosity and permittivity in terms of the phase-field variable, which results in smooth profiles of these parameters. We then utilized these in the framework described in Sect. 2 for determining the streaming potential flow with appropriate modifications to incorporate the implicit spatial dependence of the parameters. Through this framework, we are able to clearly establish that there is a sensitive interplay between the length scale of the EDL structure and that of the depleted phase. It is this interplay together with the intrinsic strength of the hydrophobic effects (captured in our framework through the specification of the contact angle) that determines the overall character of the flow. Since the overall effect of the streaming potential is to inhibit the pressure-gradient-driven flow (known as the electroviscous effect), and since the total volumetric flow rate is of tremendous importance in practical devices, we express the gross nature of the flow in terms of an effective normalized viscosity $\tilde{\eta}_{eff}$ that would result in the same (reduced) volumetric flow rate had there been only a pressure-gradient-driven flow (with no electrokinetic effects). We define: $\tilde{\eta}_{eff} = \left(\eta_{eff}/\eta_l\right) = \left(4/(3\tilde{Q})\right)$ where η_l is the viscosity of the undepleted liquid, and $\tilde{Q} = \int \tilde{u}\, \mathrm{d}y$ is the volumetric flow rate through a slit channel of height $2H$. The dependence of this effective normalized viscosity on the contact angle (representing the degree of hydrophobicity of the wall) reveals a sensitive interplay between the length scale of the EDL structure and that of the hydrophobicity-induced depletion. As shown in Fig. 2, we find that $\tilde{\eta}_{eff}$ assumes a value greater than unity (showing augmented hindrance to the flow) when the EDL is characteristically thicker than the depleted phase. For high zeta potential value, it shows an interesting transition when the length scales are equal, and it is consistently less than unity when the EDL length scale is smaller than the depleted length scale. Importantly, the thickness of the EDL is characterized by the Debye screening length, λ_l, based on the permittivity of the liquid.

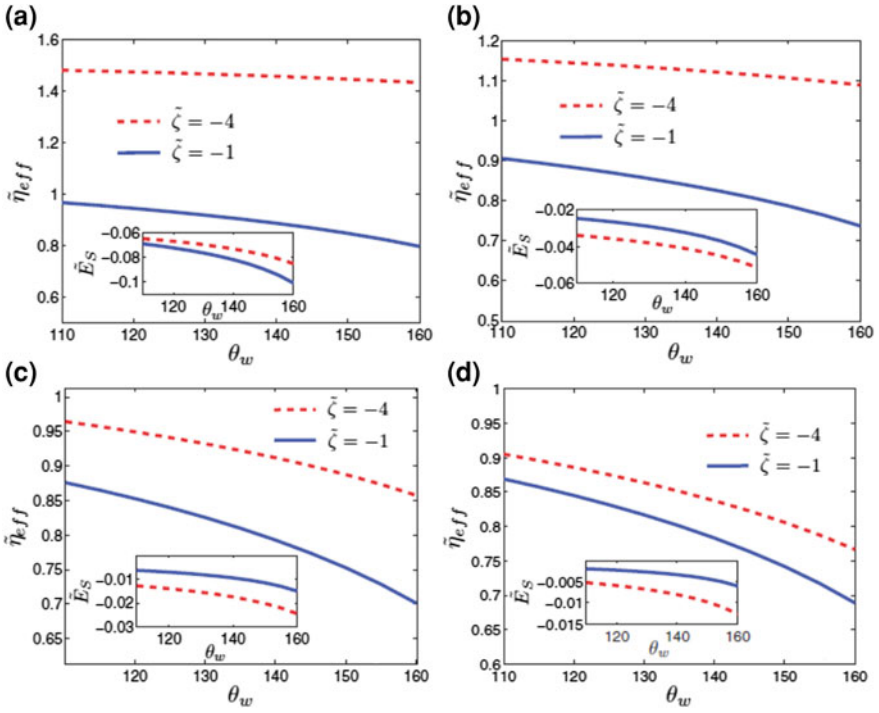

Fig. 2 Variation of the effective normalized viscosity with the contact angle for $\tilde{\zeta} = -1$, and $\tilde{\zeta} = -4$ corresponding to $H/\lambda_l = 5, 10, 25, 50$, respectively, in panels (**a**)–(**d**). The insets in each panel show the variation of the dimensionless streaming potential field with the contact angle (Reproduced from Ref. [18] with permission from the American Physical Society)

3.2 Steric Effects

It is well known that the effects of the streaming potential get progressively strong with increase in the magnitude of the zeta potential. At the same time, however, such high values of the zeta potential result in diverging values of the number density of the counterions in the near wall region as predicted by the traditional formalism described in Sect. 2 which strictly considered the ions to be point-like charges. This is taken care of by considering a modified Boltzmann approximation that incorporates the finite size of the ions—thus, precluding any potential unphysical overlap. Despite the considerably widespread use of such modified formulations, there does exist a serious theoretical inconsistency even in this modified modeling framework. This inconsistency arises from the fact that while the finite size is considered for the ionic distribution, there exists no explicit link with this finite size in the flux terms even though the diffusivity (which contributes significantly to the flux) is indeed dependent on the size of the ions. We address this fundamental theoretical issue by establishing this link [19], by using the

Stokes–Einstein relation: $D = k_B T/(6\pi\eta r)$. The need to maintain the theoretical consistency also necessitates the incorporation of the viscoelectric effect, i.e., the dependence of the dynamic viscosity on the local charge density through the relation: $1/\tilde{\eta} = 1 - \Xi$. Here, $\tilde{\eta} = \eta/\eta_0$ is the dimensionless local viscosity with η_0 being the value of the bulk viscosity, ν is the steric factor, and $\Xi = \frac{1}{2}\nu|\tilde{n}_+ - \tilde{n}_-|$. We then have $\tilde{D} = (1 - \Xi)$ where $\tilde{D} = D/D_0$ is the dimensionless diffusivity, with $D_0 = k_B T/(6\pi\eta_0 r)$ being the constant bulk value of the diffusivity. Then, by using the relation $v = 2n_0 r^3$, we may express the bulk diffusivity directly in terms of v. By using these and following the route outlined in Sect. 2, we obtain a modified expression of the streaming potential field corresponding to a fluid flow through a slit channel of height $2H$ as

$$\tilde{E}_s = \frac{3\pi\left(\frac{v}{2}\right)^{1/3}\frac{1}{\mathcal{L}_1}I_1}{I_2 - 6\pi(4v)^{1/3}\frac{\mathcal{L}_1^2}{K^2}I_3}, \tag{14}$$

where $\mathcal{L}_1 = Hn_0^{1/3}$ and $K = H/\lambda$. It can be seen in Eq. (14) that the steric effects influence both the ionic distributions and the factors responsible for determining the strength of transport of the ions. Since it is this transport that is ultimately responsible for inducing the streaming potential field, there is a far stronger dependence of this field on the finite size effects than could be envisaged within the formalism of prior theoretical treatments. Indeed, so much so that when the size is considered to be vanishingly small, i.e., $v \to 0$, the value of the streaming potential field itself becomes small. Most notably, for $\nu = 0$ representing a situation where the finite size of the ions is not considered, and is, hence, a reflection of the unmodified Boltzmann distribution which rests upon the assumption of the ions being point-like charges, no value of $\tilde{E}_s$ other than zero is possible. This seemingly nonintuitive prediction is, however, consistent with the underlying assumption of point-like charges; point entities cannot have "friction," which is inseparably present with diffusive transport, associated with them.

This conceptual understanding is clearly seen in Fig. 3. We note, in particular, that streaming potential effects may be wrongly predicted in theoretical exercises below a particular threshold of the steric factor—as indeed the plots corresponding to K = 5 and 10 show. The correct trends, i.e., higher suppression of the volumetric flow due to streaming potential for lower value of K, are seen only for $v \gtrsim \mathcal{O}(10^{-1})$. Further, as an extremely important implication of this study, we show that if one were to work consistently within the framework of the traditional Poisson-Boltzmann formalism, no value of the streaming potential other than zero is possible, as indeed seen in the figure.

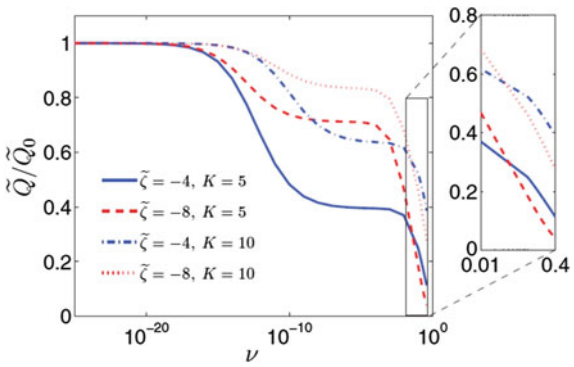

Fig. 3 Total volumetric flow rate $Q = \int_0^2 \tilde{u} d\tilde{y}$ normalized by the volumetric flow rate of the plane-Poiseuille component ($\tilde{Q}_0$) only, (i.e., $\int_0^2 (2\tilde{y} - \tilde{y}^2) d\tilde{y}$) with the steric factor, ν, corresponding to $\tilde{\zeta} = -4, 8$; for $K = 5, 10$. As ν becomes vanishingly small, $\tilde{Q}/\tilde{Q}_0 \to 1$, showing that streaming potential effects vanish in keeping with the assumption of point-like ions in the Boltzmann formalism. The magnified region shows a reversal in the trends of $\tilde{Q}/\tilde{Q}_0$ when $\nu \gtrsim \mathcal{O}(10^{-1})$, for the two different values of $\tilde{\zeta}$ (Reproduced from Ref. [19] with permission from the American Physical Society)

3.3 Thermal Effects

Most of the modeling efforts in electrokinetics, in general, and streaming potential in particular, are carried out under the assumption of isothermal conditions. This is particularly true in the micro- and nanofluidic context. This is in spite of the fact that most natural settings are non-isothermal in nature, and also that even in controlled laboratory environments, strictly isothermal conditions are difficult to realize in practice. Recognizing this, we have developed a modeling framework where thermal effects are incorporated in a comprehensive way [20]. Notably, this framework goes beyond the traditional route of a simplistic one-way coupling between the fluid flow velocity and the temperature field used in the few cases that electrokinetic flows have been studied together with thermal effects. Importantly, in this traditional route, there is no back influence of the temperature on the velocity field. Within our model, however, a complete two-way coupling is achieved by including the influence of some additional, fundamental physical phenomena. First, we include the Soret effect, which refers to the propensity of a species to move in response to a temperature gradient, with an additional term in the flux equation: $-D_{\pm} \frac{n_{\pm} q_{\pm}}{k_B T^2} \nabla T$ that immediately augments the species transport represented in Eq. (1). Here, $q_{\pm}$ denotes the ionic heat of transport of the positive, and the negative ions, and $D_{\pm}$ denotes the now temperature-dependent diffusivity of the same. Since generally, the values of q_+ and q_- are different, there is a difference in the extent to which the cations and the anions migrate in response to the temperature gradient. This generates a thermoelectric field through a

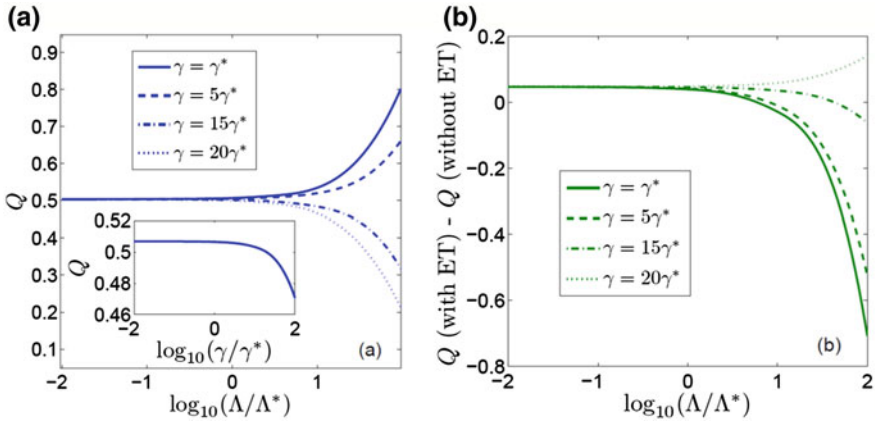

Fig. 4 Variation of the dimensionless volumetric flow rate corresponding to the variation of $\Lambda/\Lambda^* \leftarrow$ over four orders of magnitude for four different values of γ/γ^*. Inset in (**a**) shows the variation of the dimensionless volumetric flow rate with γ/γ^* varying over four orders of magnitude. In (**b**) differences in the volumetric flow rates with and without considering electrothermal effects are shown. Here, $\Lambda = q_+/(k_B T_0)$, and $\gamma = q_-/q_+$, and Λ^* and γ^* are the values of a reference alkali halide (Reproduced with slight modifications from Ref. [20] with permission from the American Physical Society)

mechanism that is analogous to the Seebeck effect. Second, we include the electrothermal effect that brings about an extra contribution to the forcing in the momentum equation due to the dependence of the permittivity on the temperature. Additionally, we incorporate the dependence of the viscosity, the thermal conductivity, and also the zeta potential on the temperature.

To study the concerted influence of these effects in a streaming potential flow, we consider again a model flow situation through a slit-channel. The thermal effects are brought about by the imposition of a linear temperature gradient on the walls.

We can observe from Fig. 4 that depending on the polarity of the generated thermoelectric field which, in turn, is determined by the relative thermo-diffusive migration strengths of the cations and the anions, the suppression of the volumetric flow rate induced by the streaming potential field may be aided or opposed. Thus, by simply imposing an external temperature gradient, we obtain extra control over the volumetric flow rate for streaming potential flows through the Soret effect and the concomitant thermoelectric field. Given a specified magnitude of the externally applied temperature gradient, we can exercise this control just by changing the nature of the electrolyte. From Fig. 4b, we can also see the role that the electrothermal effect plays in the alterations of the temperature gradient-mediated streaming potential flows. When the thermoelectric and streaming potential fields are opposing each other, this electrothermal effect basically weakens the thermoelectric field, and leads to an overall reduced flow rate compared to the case without electrothermal effects. However, when the thermoelectric and streaming

potential fields are oriented along the same direction, the consideration of the electrothermal effect enhances the overall volumetric flowrate, again by weakening the thermoelectric field. So, based on the findings of our work, it can be unambiguously inferred that temperature gradients can be successfully employed for tuning flows mediated by streaming potential.

4 Conclusions

It has been shown that flows influenced by streaming potential may be sensitively tuned by changing the hydrophobicity of the confining surfaces, as well as by exerting a temperature gradient along them. It has also been shown that a theoretically consistent model of streaming potential flows necessitates the incorporation of finite size effects in the diffusivity coefficient, too. Based on these findings, the modeling of streaming potential is being currently extended on a multitude of fronts' comprehensive framework that will emerge and be able to capture the various physicochemical phenomena in a concerted and consistent manner.

References

1. Hunter RJ (2001) Foundations of colloid science. Oxford University Press, New York
2. Quincke G (1861) Ueber die fortführung materieller Theilchen durch strömende Elektricität. Ann Phys 189:513–598
3. Delgado AV, González-Caballero F, Hunter RJ et al (2007) Measurement and interpretation of electrokinetic phenomena. J Colloid Interface Sci 309:194–224
4. Reppert PM (2000) Electrokinetics in the earth: frequency dependent electrokinetics and streaming potentials at elevated temperature and pressure. Ph.D. Thesis, Massachusetts Institute of Technology, Cambridge, Massachusetts
5. Jouniaux L, Pozzi JP (1995) Streaming potentials and permeability of saturated sandstones under triaxial stress: consequences for electrotelluric anomalies prior to earthquakes. J Geophys Res 100:10197–10209
6. Zlotnicki J, Le Mouël LL (1990) Possible electrokinetic origin of large magnetic variations at La Fournaise volcano. Nature 343:633–635
7. Riddle RC, Donahue HJ (2008) From streaming potentials to shear stress: 25 years of bone cell mechanotransduction. J Orthopaedic Res 27:143–149
8. Gu WY, Mao XG, Rawlins BA et al (1999) Streaming potential of human lumbar annulus fibrosus is anisotropic and affected by disc degeneration. J Biomech 32:1177–1182
9. Nyström M, Pihlajamäki A, Ehsani N (1994) Characterization of ultrafiltration membranes by simultaneous streaming potential and flux measurements. J Memb Sci 87:245–256
10. Chakraborty J (2013) Electrokinetics in narrow fluid fluidic confinements: the role of streaming potential. Ph.D. Thesis, Indian Institute of Technology Kharagpur, India
11. Stein D, van den Heuvel M, Dekker C (2009) Transport of ions, DNA polymers, and micrtotubules in the nanofluidic regime. In: Edel JB, deMello AJ (eds) Nanofluidics. The Royal Society of Chemistry, Cambridge, Chap 1, pp 1–30

12. Schoch RB, Han J, Renaud P (2008) Transport phenomena in nanofluidics. Rev Mod Phys 80:839–883
13. Sparreboom W, van den Berg A, Eijkel JCT (2009) Principles and applications of nanofluidic transport. Nat Nanotechnol 4:713–720
14. Squires TM, Quake SR (2005) Microfluidics: fluid physics at the nanoliter scale. Rev Mod Phys 77:977–1026
15. Stone HA, Stroock AD, Ajdari A (2004) Engineering flows in small devices: microfluidics toward a lab-on-a-chip. Ann Rev Fluid Mech 36:381–411
16. Zhao C, Yang C (2012) Advances in electrokinetics and their applications in micro/nano fluidics. Microfluid Nanofluid 13:179–203
17. Stone HA (2002) Partial differential equations in thin film flows in fluid dynamics: spreading droplets and rivulets. In: Berestycki H, Pomeau Y (eds) Nonlinear PDEs in condensed matter and reactive flows. Kluwer, Dordrecth
18. Chakraborty J, Chakraborty S (2013) Influence of hydrophobic effects on streaming potential. Phys Rev E 88:043007
19. Chakraborty J, Dey R, Chakraborty S (2012) Consistent accounting of steric effects for prediction of streaming potential in narrow confinements. Phys Rev E 86:061504
20. Ghonge T, Chakraborty J, Dey R et al (2013) Electrohydrodynamics within the electrical double layer in the presence of finite temperature gradients. Phys Rev E 88:053020